Research Article

Journal of Applied Toxicology

Received: 24 September 2014, Revised: 20 October 2014, Accepted: 3 November 2014 Published online in Wiley Online Library: 6 February 2015

(wileyonlinelibrary.com) DOI 10.1002/jat.3097

Comparative cytotoxicity of dolomite nanoparticles in human larynx HEp2 and liver HepG2 cells

Maqusood Ahamed[a]*, Hisham A. Alhadlaq[b], Javed Ahmad[c], Maqsood A. Siddiqui[c], Shams T. Khan[c], Javed Musarrat[d] and Abdulaziz A. Al-Khedhairy[c]

ABSTRACT: Dolomite is a natural mineral of great industrial and commercial importance. With the advent of nanotechnology, natural minerals including dolomite in the form of nanoparticles (NPs) are being utilized in various applications to improve the quality of products. However, safety or toxicity information of dolomite NPs is largely lacking. This study evaluated the cytotoxicity of dolomite NPs in two widely used *in vitro* cell culture models: human airway epithelial (HEp2) and human liver (HepG2) cells. Concentration-dependent decreased cell viability and damaged cell membrane integrity revealed the cytotoxicity of dolomite NPs. We further observed that dolomite NPs induce oxidative stress in a concentration-dependent manner, as indicated by depletion of glutathione and induction of reactive oxygen species (ROS) and lipid peroxidation. Quantitative real-time PCR data demonstrated that the mRNA level of tumor suppressor gene p53 and apoptotic genes (bax, CASP3 and CASP9) were up-regulated whereas the anti-apoptotic gene bcl-2 was down-regulated in HEp2 and HepG2 cells exposed to dolomite NPs. Moreover, the activity of apoptotic enzymes (caspase-3 and caspase-9) was also higher in both kinds of cells treated with dolomite NPs. It is also worth mentioning that HEp2 cells seem to be marginally more susceptible to dolomite NPs exposure than HepG2 cells. Cytotoxicity induced by dolomite NPs was efficiently prevented by N-acetyl cysteine treatment, which suggests that oxidative stress is primarily responsible for the cytotoxicity of dolomite NPs in both HEp2 and HepG2 cells. Toxicity mechanisms of dolomite NPs warrant further investigations at the *in vivo* level. Copyright © 2015 John Wiley & Sons, Ltd.

Keywords: dolomite nanoparticles; human health; cytotoxicity; oxidative stress; apoptosis

Introduction

Dolomite is a natural mineral composed of calcium magnesium carbonate [$CaMg(CO_3)_2$]. Usually minerals are named after a geographic locality where they occur, however, dolomite was named after French geologist Deodat de Dolomieu (1750–1801) (Janez, 2001). Dolomite is an important raw material used in various applications including road and building construction materials, glass manufacturing, metallurgy, and ceramic glazes (British Geological Survey) on Dolomites, 2006; Roberts, 1981). Dolomite is relatively soft and easily crushed to a fine powder, which is used as agricultural lime by farmers to reduce soil acidity and also to adjust magnesium deficiencies (Chen *et al*., 2006). Dolomite is also used for a range of filler applications in plastics, paints, rubbers and adhesives (BGS (British Geological Survey) on Dolomites, 2006). Dolomite is even utilized in cosmetics such as facial creams, baby powder and toothpaste (Slomski and Odle, 2005). More importantly, dolomite is being used for its potential ability to act as a calcium and magnesium supplement (Mizoguchi *et al*., 2005), although its safety and effectiveness as such has yet to proven. With the advent of nanotechnology, many natural minerals in the form of nanoparticles (NPs, 1–100 nm) are being utilized in various industrial and commercial applications to improve the quality of products (Akhtar *et al*., 2014; Berlo *et al*., 2009; Buseck and Pósfai, 1999; Hochella *et al*., 2008). Therefore, an improved understanding of the potential risks, comprising of exposure and hazard assessments, associated with exposure to such NPs is necessary to check its toxicity or safety (Kim *et al*., 2011; Maynard *et al*., 2006).

The materials at nano-scale shows new and different properties compared with what they exhibit on a macro-scale, enabling unique applications (Jos *et al*., 2009; Oberdorster *et al*., 2005). The unique physicochemical properties of NPs come from their high surface-area-to-volume ratio. They also have a considerably higher percentage of atoms on their surface compared with bulk particles, which can make them more reactive. These

*Correspondence to: Maqusood Ahamed, King Abdullah Institute for Nanotechnology, King Saud University, Riyadh 11451, Saudi Arabia.
Email: maqusood@gmal.com

[a]King Abdullah Institute for Nanotechnology, King Saud University, Riyadh 11451, Saudi Arabia

[b]Department of Physics and Astronomy, College of Science, King Saud University, Riyadh 11451, Saudi Arabia

[c]Department of Zoology, College of Science, King Saud University, Riyadh 11451 Saudi Arabia

[d]Department of Agricultural Microbiology, Faculty of Agricultural Sciences, Aligarh Muslim University, Aligarh 202002, India

Journal of Applied Toxicology

characteristics are only present at the nano-scale level and have thus led to its heightened experimentation and use in modern industries. However, these unique characteristics of NPs may also pose adverse human and environmental health effects (Avalos *et al*., 2014; Maynard and Kuempel, 2005). The nano size of these particles renders them the ability to be easily transported into biological systems, thus raising the question of their effects on the susceptible system. Recently, researchers started focusing attention on the toxicity of natural minerals at a nano-scale level (Medical Research, 2012; Patil *et al*., 2012; Plathe *et al*., 2013). Patil *et al*. (2012) reported that dolomite NPs induced higher cytotoxicity than microparticles in human lung epithelial A549 cells. The authors suggested that separate health safety standards would be required for nano-scale dolomite particles. Understanding the toxicity of dolomite NPs at a cellular and molecular level is important for the rational design of this material for diverse applications.

The potential mechanisms of toxicity of nano-scale materials are still not fully explored. One mechanism often discussed is the depletion of antioxidants including glutathione and protein bound sulfhydryl groups and the induction of oxidants such as lipid peroxidation (LPO) and reactive oxygen species (ROS) generation have been implicated in oxidative damage of cell molecules (Ahamed *et al*., 2010, 2013). ROS are important factors not only in apoptotic cell death, but also in DNA damage and many other cellular processes (Guo and Wang, 2009; Patlolla *et al*., 2010). Apoptotic cell death is regulated by various genes acting as death switches. Tumor suppressor gene p53 is able to activate cell-cycle checkpoints, DNA repair and apoptosis to maintain genomic stability (Sherr, 2004). The ratio of bax/bcl-2 proteins represents a cell death switch, which determines the life or death of cells in response to an apoptotic stimulus; an increased bax/bcl-2 ratio decreases the cellular resistance to apoptotic stimuli, leading to apoptosis (Chougule *et al*., 2011). Moreover, destabilization of mitochondrial integrity by apoptotic stimuli precedes activation of caspases leading to apoptosis (Youle and Strasser, 2008).

The exposure of NPs could occur through the respiratory tract, dermal contact or gastrointestinal tract (Oberdorster *et al*., 2005). Thus, it is important to investigate the toxicity of dolomite NPs in relevant human tissues. We have chosen two widely used *in vitro* cell culture models, human larynx HEp2 cells and human liver HepG2 cells, as tools for assessing the potential cytotoxicity of dolomite NPs. The human laryngeal epithelial HEp2 cells were used because the respiratory tract represents the main exposure route for workers employed in the production and handling of NPs as well as environmental exposure to the general population. NPs have a potentially high efficiency for deposition in the respiratory tract both in the upper and the lower part for a long time where they induce oxidative stress and inflammation (Madl and Pinkerton, 2009). Human liver HepG2 cells were utilized because the liver is a primary site of NPs accumulation after they gain entry into the body through any of the possible routes of exposure (Johnston *et al*., 2009; Kim *et al*., 2008; Wang *et al*., 2008). Both types of cell lines (HEp-2 and HepG2) have been widely used in toxicological studies (Fahmy and Cormier, 2009; Piret *et al*., 2012; Siddiqui *et al*., 2012)

The main objective of this study was to investigate how dolomite NPs interacts with two different human cells (HEp2 and HepG2) in order to understand the impact of such nano-scale materials on cellular systems. In addition, the effects of dolomite NPs on oxidative stress markers, the mitochondrial membrane potential and apoptotic genes were evaluated to explore the feasible mechanisms of dolomite NPs induced cytotoxicity.

Materials and Methods

Chemical and Reagents

Dulbecco's modified eagle's medium (DMEM), hank's balanced salt solution (HBSS), fetal bovine serum (FBS) and penicillin–streptomycin were bought from Invitrogen Co. (Carlsbad, CA, USA). N-acetyl cysteine (NAC), 3-(4, 5-dimethylthiazol-2-yl)-2, 5-diphenyltetrazoliumbromide (MTT), 3-amino-7-dimethylamino-2-methyl-phenazine hydrochloride (neutral red), Rhodamine-123 dye (Rh123) and 2, 7-dichlorofluorescin diacetate (DCFH-DA) were purchased from Sigma-Aldrich (St. Louis, MO, USA). Caspase-3 and −9 enzymes assays and LDH assay kits were purchased from Bio-Vision Inc. (Milpitas, CA, USA). All other chemicals used were of the highest purity available from commercial sources.

Dolomite Nanoparticles

Dolomite nanopowder was a kind gift from Dr Iqbal Ahmad (CSIR-Indian Institute of Toxicology Research, Lucknow, India). Dolomite NPs were prepared by grinding the micro-particles of dolomite in a ball mill (PM 100; Retsch, Haan, Germany), at alternative cycles of grinding (5 min) and halt (10 min) at 326 g using the mixtures of different sizes of balls. It took approximately 48 h to get NPs of dolomite. Morphology and size of NPs were determined by transmission electron microscopy (TEM), scanning electron microscopy (SEM) and dynamic light scattering (DLS).

Electron Microscopy Characterization of Dolomite Nanoparticles

The shape, size and surface morphology of dolomite NPs were determined by field emission scanning electron microscope (FESEM, JSM-7600 F; JEOL Inc., Tokyo, Japan) and field emission transmission electron microscopy (FETEM, JEM-2100 F; JEOL Inc.) at an accelerating voltage of 15 and 200 kV, respectively. For TEM measurements, the dry powder of dolomite NPs was suspended in de-ionized water at a concentration of 1 mg ml^{-1}, and then sonicated using a sonicator bath at room temperature for 15 min at 40 W to form a homogeneous suspension. For size measurement, sonicated 1 mg ml^{-1} dolomite NPs stock solution was then diluted to an appropriate working solution. Further, a drop of aqueous dolomite NPs suspension was placed onto a carbon-coated copper grid, air dried and observed with FETEM.

Dynamic Light Scattering Characterization of Dolomite Nanoparticles

The average hydrodynamic size and zeta potential of dolomite NPs in de-ionized water and cell culture medium were examined by DLS (Nano-ZetaSizer-HT, Malvern, UK) as described by Murdock *et al*. (2008). In brief, a dry powder of dolomite NPs was suspended in de-ionized water and complete cell culture medium (DMEM with 10% FBS) at a concentration of 80 μg ml^{-1} for 24 h. Then, the suspension was sonicated using a sonicator bath at room temperature for 15 min at 40 W and the DLS

experiments performed. We have utilized 80 μg ml^{-1} for DLS measurement because this is the maximum exposure level used in cytotoxicity studies.

Cell Culture and Nanoparticles Exposure

HepG2 and HEp2 cells were obtained from American Type Culture Collection (ATCC) (Manassas, VA, USA). Cells were cultured in DMEM medium supplemented with 10% FBS and 100 U ml^{-1} penicillin–streptomycin at 5% CO_2 and 37 °C. At 85% confluence, cells were harvested using 0.25% trypsin and were sub-cultured into 25-cm^2 flasks, 6-well plates or 96-well plates according to selection of the experiments. Cells were allowed to attach to the surface for 24 h prior to treatment. The dry powder of dolomite NPs was suspended in cell culture medium at a concentration of 1 mg ml^{-1} and diluted to appropriate concentrations (1–80 μg ml^{-1}). The dilutions of dolomite NPs were then sonicated using a sonicator bath at room temperature for 15 min at 40 W to avoid NPs agglomeration prior to cell exposure. Under some conditions, HepG2 and HEp2 cells were pre-exposed for 1 h with 10 mM of NAC before 24 h co-exposure with or without dolomite NPs. Cells not exposed to dolomite NPs served as controls in each experiment.

MTT Assay

The MTT cell viability assay was carried according to the procedure as described by Mossman (1983) with some modifications (Ahamed *et al.*, 2011). This assay assesses the mitochondrial function by measuring the ability of viable cells to reduce MTT into blue formazon product. In brief, 1×10^4 cells per well were seeded in 96-well plates and exposed to different concentrations of dolomite NPs (1–80 μg ml^{-1}) for 24 h. At the end of the exposure time, culture medium was removed from each well to avoid interference of NPs and replaced with new medium containing MTT solution in an amount equal to 10% of culture volume and incubated for 3 h at 37 °C until a purple-colored formazan product developed. The resulting formazan product was dissolved in acidified isopropanol. After this the 96-well plate was centrifuged at 2300 *g* for 5 min to settle down the remaining NPs present in the solution. Then, 100 μl supernatant was transferred to new 96-well plate, and the absorbance was measured at 570 nm using a microplate reader (Synergy-HT; BioTek, Winooski, VT, USA).

NRU Assay

The neutral red uptake (NRU) assay was performed according to the procedure described by Borenfreund and Puerner (1984) with some modifications (Ahamed *et al.*, 2011). In brief, 1×10^4 cells per well were seeded in 96-well plates and exposed to different concentrations of dolomite NPs (1–80 μg ml^{-1}) for 24 h. At the end of the exposure time, the test solution was aspirated and cells were washed with phosphate-buffer saline (PBS) twice before being incubated for 3 h in medium supplemented with neutral red (50 μg ml^{-1}). The medium was washed off rapidly with a solution containing 0.5% formaldehyde and 1% calcium chloride. The cells were then incubated for a further 20 min at 37 °C in a mixture of acetic acid (1%) and ethanol (50%) to extract the dye. The 96-well plate was then centrifuged at 2300 *g* for 5 min to settle down the remaining NPs present in the solution. After this the 100-μl supernatant was transferred to a new 96-well plate and the absorbance was measured at 540 nm using the microplate reader (Synergy-HT; BioTek).

LDH Assay

The LDH assay was carried out using a BioVision LDH-cytotoxicity colorimetric assay kit according to the manufacturer's protocol. In brief, 1×10^4 cells per well were seeded in 96-well plates and exposed to different concentrations of dolomite NPs (1–80 μg ml^{-1}) for 24 h. After the exposure period had elapsed, each 96-well plate was centrifuged at 2300 *g* for 5 min to settle the NPs present in the solution. Then 100 μl of the supernatant was transferred to new 96-well plate that already contained 100 μl of the reaction mixture from the BioVision kit and incubated for 30 min at room temperature. At the end of incubation time, the absorbance of the solution was measured at 340 nm using the microplate reader (Synergy-HT; BioTek). The LDH levels in the culture medium versus those in the cells were quantified and compared with the control values according to the manufacturer's instructions

ROS Assay

Intracellular ROS generation after dolomite NPs exposure was measured using 2,7-dichlorofluorescin diacetate (DCFH-DA) as described by Wang and Joseph (1999) with some modifications (Siddiqui *et al.*, 2013). Generation of ROS was determined using two methods: fluorometric analysis and microscopic fluorescence imaging. For fluorometric analysis, cells (1×10^4 cells per well) were seeded in 96-well black-bottomed culture plates and allowed to adhere for 24 h in a CO_2 incubator at 37 °C. Next, the cells were exposed to different concentrations of dolomite NPs (10–80 μg ml^{-1}) for 24 h. At the end of the exposure time, cells were washed twice with HBSS before being incubated in 1 ml of working solution of DCFH-DA at 37 °C for 30 min. After this, the cells were lysed in alkaline solution and centrifuged at 2300 *g* for 10 min. A 200-μl supernatant was transferred to a new 96-well plate, and fluorescence was measured at 485 nm excitation and 520 nm emission using the microplate reader (Synergy-HT; BioTek). The values were expressed as a percent of fluorescence intensity relative to the control wells.

A parallel set of cells (5×10^4 cells/well in a 24-well transparent plate) were analyzed for intracellular fluorescence using a fluorescence microscope (Olympus CKX 41; Olympus: Center Valley, Pennyslvania, USA), with images taken at 20× magnification.

Preparation of Crude Cell Extract

We have prepared crude cell extract for the assay of lipid peroxidation (LPO), glutathione (GSH) and caspase enzymes, as described in our previous publication (Ahmad *et al.*, 2012). In brief, cells were cultured in a 75-cm^2 culture flask and exposed to different concentrations of dolomite NPs (10–80 μg ml^{-1}) for 24 h. At the end of the exposure time, cells were harvested in ice-cold PBS by scraping and washed with PBS at 4 °C. The cell pellets were then lysed in cell lysis buffer [1× 20 mM Tris–HCl (pH 7.5), 150 mM NaCl, 1 mM Na_2EDTA, 1% Triton, 2.5 mM sodium pyrophosphate]. After centrifugation (15 000 *g* for 10 min at 4 °C) the supernatant (cell extract) was maintained on ice for further assays.

Journal of Applied Toxicology

LPO Assay

LPO was estimated by measuring the formation of malondialdehyde (MDA) using the method of Ohkawa *et al.* (1979). MDA is one of the end products of LPO. Briefly, a mixture of 0.1 ml of crude cell extract and 1.9 ml of 0.1 M sodium phosphate buffer (pH 7.4) was incubated at 37 °C for 1 h. After incubation, mixture was precipitated with 5% TCA and centrifuged (2300 *g* for 15 min at room temperature) to collect the supernatant. Then 1.0 ml of 1% TBA was added to the supernatant and placed in boiling water for 15 min. After cooling to room temperature the absorbance of the mixture was taken at 532 nm and was converted to MDA and expressed in terms of percentage as compared with the control.

GSH Assay

The GSH level was quantified using Ellman's (1959) method. Briefly, a mixture of 0.1 ml of crude cell extract and 0.9 ml of 5% TCA was centrifuged (2300 *g* for 15 min at 4 °C). Then 0.5 ml of the supernatant was added into 1.5 ml of 0.01% DTNB and the reaction was monitored at 412 nm. The amount of GSH was expressed in terms of percentage as compared with the control.

MMP Assay

The mitochondrial membrane potential (MMP) was measured according to the protocol of Zhang *et al.* (2011) with some modifications (Ahamed and Alhadlaq, 2014). In brief, cells (5×10^4 cells per well) were treated with different concentrations (10–80 $\mu g\,ml^{-1}$) of dolomite NPs for 24 h. At the end of the exposure time, cells were harvested and washed twice with PBS. Cells were further exposed to 10 $\mu g\,ml^{-1}$ Rh-123 fluorescent dye for 1 h at 37 °C in the dark. Again, cells were washed twice with PBS then the fluorescence intensity of the Rh-123 dye was measured using an upright fluorescence microscope (OLYMPUS CKX 41) by capturing the images at 20× magnification.

A parallel set of cells (1×10^4 cells per well) in a 96-well plate were analyzed for quantification of Rh-123 using the microplate reader (Synergy-HT; BioTek).

Quantitative Real-Time PCR Analysis

Cells were cultured in six-well plates and exposed to dolomite NPs at a concentration of 40 $\mu g\,ml^{-1}$ for 24 h. At the end of the exposure time, total RNA was extracted using the Qiagen RNeasy mini Kit (Valencia, CA, USA) according to the manufacturer's instructions. The concentration of the extracted RNA was determined using a Nanodrop 8000 spectrophotometer (Thermo-Scientific, Wilmington, DE, USA), and the integrity of RNA was visualized on 1% agarose gel using the gel documentation system (Universal Hood II; BioRad, Hercules, CA, USA). The first strand of cDNA was synthesized from 1 μg of total RNA by the reverse transcriptase using M-MLV (Promega, Madison, WI, USA) and oligo (dT) primers (Promega) according to the manufacturer's protocol. Quantitative real-time PCR was performed using the QuantiTect SYBR Green PCR kit (Qiagen) using the ABI PRISM 7900HT Sequence Detection System (Applied Biosystems, Foster City, CA, USA). Two microliters of template cDNA was added to the final volume of 20 μl of reaction mixture. Real-time PCR cycle parameters included 10 min at 95 °C followed by 40 cycles involving denaturation at 95 °C for 15 s, annealing at 60 °C for 20 s and elongation at 72 °C for 20 s. The sequences of the specific sets of primer for p53, bax, bcl-2, caspase-3 (CASP3), caspase-9 (CASP9) and β-actin used in this study are given in our previous publication (Ahamed *et al.*, 2011). Expressions of selected genes were normalized to the β-actin gene, which was used as an internal housekeeping control.

Caspase-3 and Caspase-9 Enzymes Assay

Activity of caspase-3 and caspase-9 enzymes was examined in treated and control cells using Bio-Vision colorimetric assay kits. Crude cell extract was prepared as described above. This assay is based on the principle that activated caspases in apoptotic cells cleave the synthetic substrates to release free chromophore p-nitroanilide (pNA), which is measured at 405 nm. The pNA was generated after specific action of caspase-3 and caspase-9 on tertrapeptide substrates DEVD-pNA and LEHD-pNA, respectively (Ahamed *et al.*, 2011; Berasain *et al.*, 2005). The reaction mixture consisted of 50 μl of cell extract protein (as prepared above), 50 μl of 2× reaction buffer (containing 10 mM dithiothreitol) and 5 μl of 4 mM DEVD-pNA (for caspase-3) or LEHD-pNA (for caspase-9) substrate in a total volume of 105 μl. The reaction mixture was incubated at 37 °C for 1 h and absorbance of the product was measured using the microplate reader (Synergy-HT; BioTek) at 405 nm according to manufacturer's protocol.

Protein Assay

The total protein content in the cell extracts was estimated by the Bradford method (Bradford, 1976) using bovine serum albumin as the standard.

Statistical Analysis

Statistical significance was determined by one-way analysis of variance followed by Dunnett's multiple comparison tests. Significance was ascribed at $P < 0.05$.

Results

Characterization of Dolomite Nanoparticles

We have utilized FETEM, FESEM and DLS techniques to characterize the dolomite NPs. Figure 1A shows the typical TEM image of dolomite NPs. High-resolution TEM suggested the crystalline nature of these particles (Fig. 1B). The SEM image depicts the surface morphology dolomite NPs (Fig. 1C). TEM and SEM images show that particles were agglomerated. We never found small independent crystals in these pictures. The TEM average diameter was calculated from measuring over 100 particles in random fields of view. The average diameter of dolomite NPs was around 13 nm. Figure 1D represents the frequency of size distribution of dolomite NPs.

DLS characterization of dolomite NPs is given in Table 1. The hydrodynamic size of dolomite NPs in de-ionized water and cell culture medium was 283 and 237 nm, respectively. Further, the zeta-potential of dolomite NPs in water and culture medium was −16 and −21 mV, respectively.

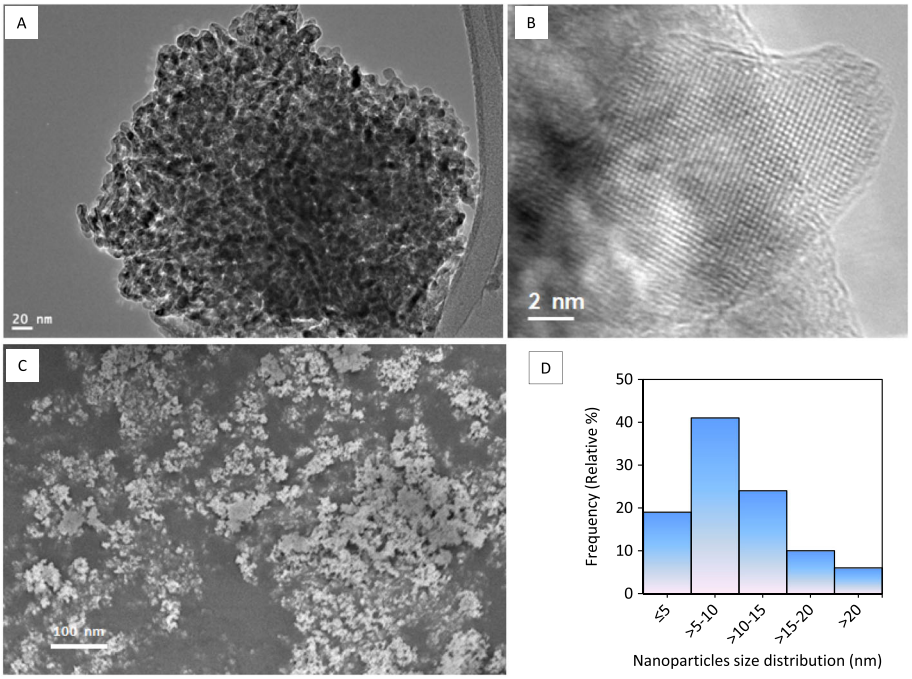

Figure 1. Electron microscopy characterization of dolomite nanoparticles (NPs). (A) Field emission transmission electron microscopy (FETEM) image, (B) FETEM image with high resolution, (C) field emission scanning electron microscope (FESEM) image and (D) frequency of particle size distribution.

Table 1. Dynamic light scattering (DLS) characterization of dolomite nanoparticles (NPs)

DLS characterization of dolomite NPs		
	De-ionized water (mean ± SD)	Culture media (mean ± SD)
Hydrodynamic size (nm)	283 ± 73	237 ± 47
Zeta potential (−mV)	16 ± 5	21 ± 3

Dolomite Nanoparticles Induced Cytotoxicity

HepG2 and HEp2 cells were exposed to different concentrations (1–80 μg ml^{-1}) of dolomite NPs for 24 h and cytotoxicity was evaluated by the MTT, NRU and LDH assays. All three assays have shown that dolomite NPs up to the concentration of 5 μg ml^{-1} did not produce significant cytotoxicity ($P > 0.05$ for each). As the concentration of NPs increased to 10, 20, 40 and 80 μg ml^{-1} cytotoxicity was observed in a concentration-dependent manner. MTT results showed that viability of HepG2 cells was decreased to 83%, 72%, 60% and 54%, whereas HEp2 cell viability reduction was 76%, 69%, 54% and 46% at the concentrations of 10, 20, 40 and 80 μg ml^{-1}, respectively ($P < 0.05$ for each) (Fig. 2A). Figure 2B shows the results of cell viability obtained by the NRU assay. NRU data were consistent with MTT results.

We further observed that dolomite NPs induced LDH leakage concentration dependently in both types of cells. LDH leakage in HepG2 cells increased to 117%, 135%, 169% and 199%, whereas in HEp2 cells LDH leakage was increased to 132%, 149%, 187% and 214% for the concentrations of 10, 20, 40 and 80 μg ml^{-1}, respectively ($P < 0.05$ for each) (Fig. 2A). Moreover, an inverse linear correlation was observed between LDH leakage and MTT cell viability in HepG2 ($R2 = 0.9344$) and HEp2 ($R2 = 0.9721$) cells (Fig. 3A, B).

Dolomite Nanoparticles Induced Oxidative Stress

Oxidative stress has been suggested to be involved in mutagenicity, DNA damage and apoptosis (Nel *et al.*, 2006; Ott *et al.*, 2007). We examined the potential of dolomite NPs to induce oxidative stress by measuring the ROS, LPO and GSH levels in HepG2 and HEp2 cells. Quantitative data suggested that dolomite NPs induced intracellular ROS generation in a concentration-dependent manner ($P < 0.05$ for each) (Fig. 4A). Fluorescent microscopy data also revealed that dolomite NPs-treated cells express a high intensity of green fluoresce DCF dye (marker of ROS generation) as compared with the control (Fig. 4B). The MDA level, an end product of LPO, was significantly higher, whereas the antioxidant GSH level was significantly lower in a concentration-dependent manner in HepG2 and HEp2 cells exposed to dolomite NPs (Fig. 5A, B).

Dolomite Nanoparticles Induced MMP Loss

It has been reported in the scientific literature that mitochondrial membrane potential (MMP) decreases during apoptotic cell death (Sharma *et al.*, 2012). Dolomite NPs-induced MMP loss in HepG2 and HEp2 cells was recorded in terms of fluorescence intensity of mitochondrial-specific dye Rh-123. A concentration-dependent decrease in Rh-123 fluorescent intensity was observed in cells exposed to different concentrations of dolomite NPs (10–80 μg ml^{-1}) (Fig. 6A). Fluorescence microscopy data also supported the quantitative results. The brightness of the fluorescent intensity was reduced in cells exposed to dolomite NPs that indicates a significant reduction in MMP (Fig. 6B).

Journal of Applied Toxicology

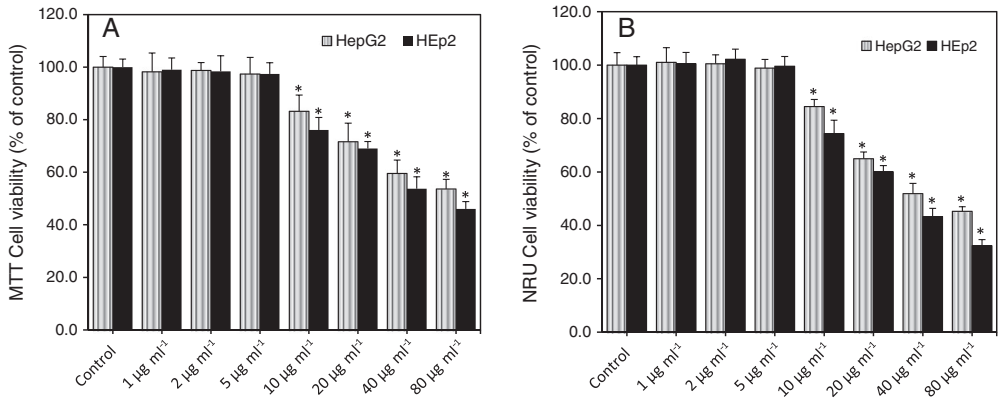

Figure 2. Dolomite nanoparticles (NPs) reduced the viability of HepG2 and HEp2. Cells were exposed to different concentrations (1–80 μg ml^{-1}) of dolomite NPs for 24 h. At the end of the exposure, cell viability was determined as described in the *Materials and Methods*. (A) Mitochondrial function (MTT) assay and (B) lysosomal activity (NRU) assay. Data represented are the mean ± SD of three identical experiments made in three replicate. *Significant difference as compared with the controls ($P < 0.05$ for each).

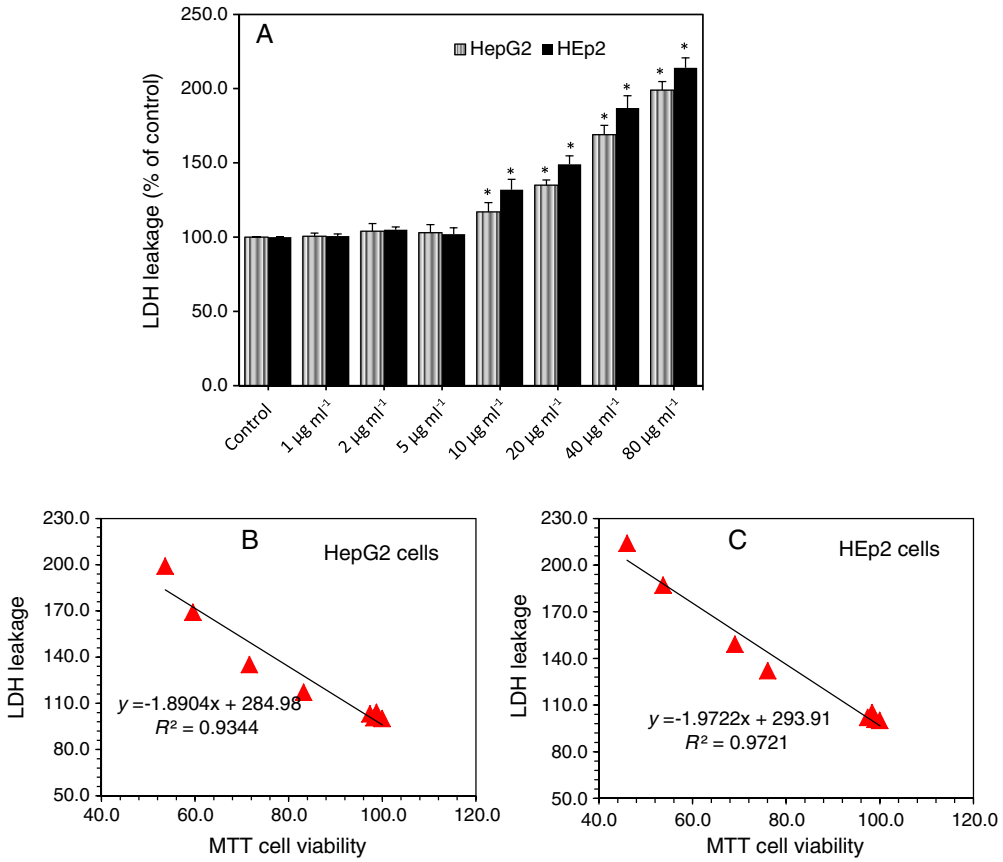

Figure 3. Dolomite nanoparticles (NPs) induced membrane damage in HepG2 and HEp2. Cells were exposed to different concentrations (1–80 μg ml^{-1}) of dolomite NPs for 24 h. At the end of the exposure, membrane damage was determined as described in materials and methods. (A) Membrane integrity (LDH) assay. Data represented are the mean ± SD of three identical experiments made in three replicate. *Significant difference as compared with the controls ($P < 0.05$ for each). A significant negative correlation between the MTT cell viability and LDH leakage in HepG2 (B) and HEp2 (C) cells after dolomite NPs exposure.

Dolomite Nanoparticles Induced Apoptosis

We have utilized quantitative real-time PCR to analyze the mRNA level of several genes involved in apoptosis (p53, bax, bcl-2, CASP3 and CASP9) in HepG2 and HEp2 cells treated with dolomite NPs at a concentration of 40 μg ml^{-1} for 24 h. The results showed that dolomite NPs significantly altered the regulation of these genes in both types of cells ($P < 0.05$ for each) (Fig. 7A). The mRNA expression levels of the cell-cycle checkpoint gene p53 and pro-apoptotic gene bax were up-regulated whereas the expression of the anti-apoptotic gene bcl-2 was down-

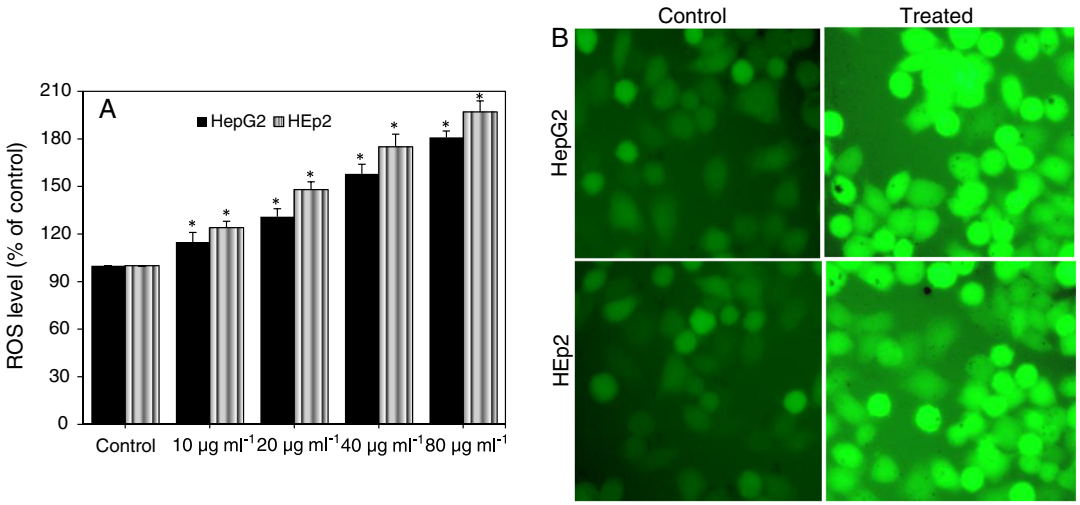

Figure 4. Dolomite NPs induced reactive oxygen species (ROS) generation in HepG2 and HEp2 cells. (A) Percentage change in ROS generation in HepG2 and HEp2 cells after dolomite nanoparticle (NPs) exposure at the concentrations of 0, 10, 20, 40 and 80 μg ml^{-1} for 24 h. Data represented are the mean ± SD of three identical experiments made in three replicate. *Statistically significant difference as compared with the control (P <0.05). (B) Representative microphotographs showing ROS generation in HepG2 and HEp2 cells after dolomite NPs exposure at a concentration of 80 μg ml^{-1} for 24 h. Images were captured with a fluorescence microscope (Olympus CKX 41).

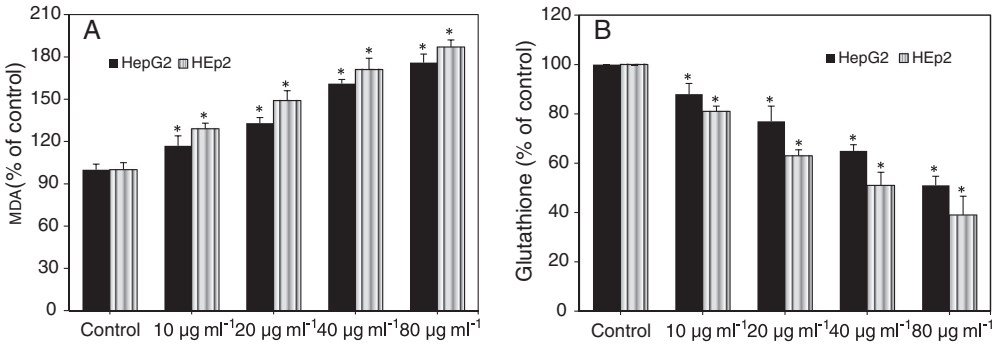

Figure 5. Dolomite nanoparticles (NPs) induced malondialdehyde (MDA) levels and depleted glutathione (GSH) levels in HepG2 and HEp2 cells. Cells were exposed to different concentrations (1–80 μg ml^{-1}) of dolomite NPs for 24 h. At the end of the exposure, MDA and GSH levels were determined as described in the *Materials and Methods*. (A) MDA level and (B) GSH level. Data represented are the mean ± SD of three identical experiments made in three replicate. *Significant difference as compared with the controls (P <0.05 for each).

regulated in cells exposed to dolomite NPs. We also observed the higher expression of CASP3 and CASP9 genes in treated cells than those of the control.

To confirm the quantitative real-time PCR data, we further evaluated the activity of caspase-3 and caspase-9 enzymes in HepG2 and HEp2 cells exposed to dolomite NPs at a concentration of 40 μg ml^{-1} for 24 h. We observed that dolomite NPs significantly increased the activity of both apoptotic enzymes (caspas-3 and caspase-9) in HEp2 and HepG2 cells (P <0.05 for each) (Fig. 7B).

Cytotoxicity of Dolomite Nanoparticles was Mediated Through Oxidative Stress

In order to investigate whether oxidative stress could play a critical role in cytotoxicity of dolomite NPs, HepG2 and HEp2 cells were exposed to dolomite NPs in the presence of NAC, a potent ROS scavenger. Results showed that NAC significantly prevented the ROS generation as well as abolished almost fully the cytotoxic effect of dolomite NPs in both types of cells (Fig. 8A, B).

Taken together, our data demonstrated that cytotoxicity, oxidative stress and the apoptotic response of dolomite NPs were slightly higher in HEp2 cells as compared with HepG2 cells. However, the mode of action of cytotoxicity of dolomite NPs was similar in both HEp2 and HepG2 cells.

Discussion

The toxic effects of mineral NPs have been considered as a serious limitation for their diverse applications and prior toxicological characterization of these NPs are needed. NPs may pose adverse effects because of their small size and unique physiochemical characteristics (Mahmood *et al*., 2010; Murdock *et al*., 2008). Therefore, it is necessary to characterize the selected NPs before their biological studies. The principal parameters of NPs are their shape, size, crystal structure, purity, hydrodynamic size and aggregation that regulate the biological response of NPs (Nel *et al*., 2006; Yu *et al*., 2009). We have employed TEM, SEM and DLS techniques to characterize the dolomite NPs. The primary particle size of dolomite determined by TEM was around 13 nm. High-resolution TEM images suggested the crystalline

Journal of Applied Toxicology

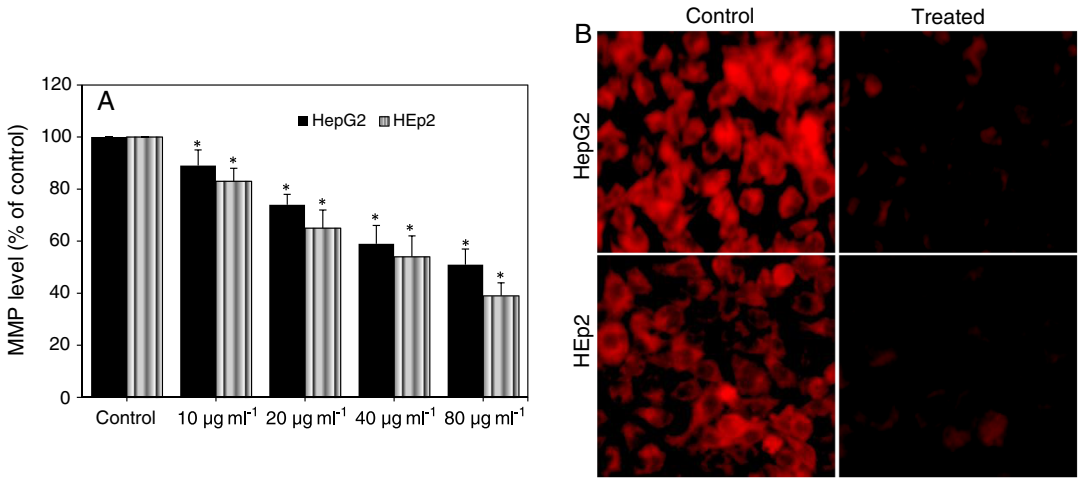

Figure 6. Dolomite nanoparticles (NPs) induced mitochondrial membrane potential (MMP) loss in HepG2 and HEp2 cells. (A) Percentage change in MMP in HepG2 and HEp2 cells after dolomite NPs exposure at the concentrations of 0, 10, 20, 40 and 80 μg ml^{-1} for 24 h. Data represented are the mean ± SD of three identical experiments made in three replicate. *Statistically significant difference with compared with the control (P <0.05). (B) Representative microphotographs showing MMP loss in HepG2 and HEp2 cells after dolomite NPs exposure at a concentration of 80 μg ml^{-1} for 24 h. Images were captured with a fluorescence microscope (Olympus CKX 41).

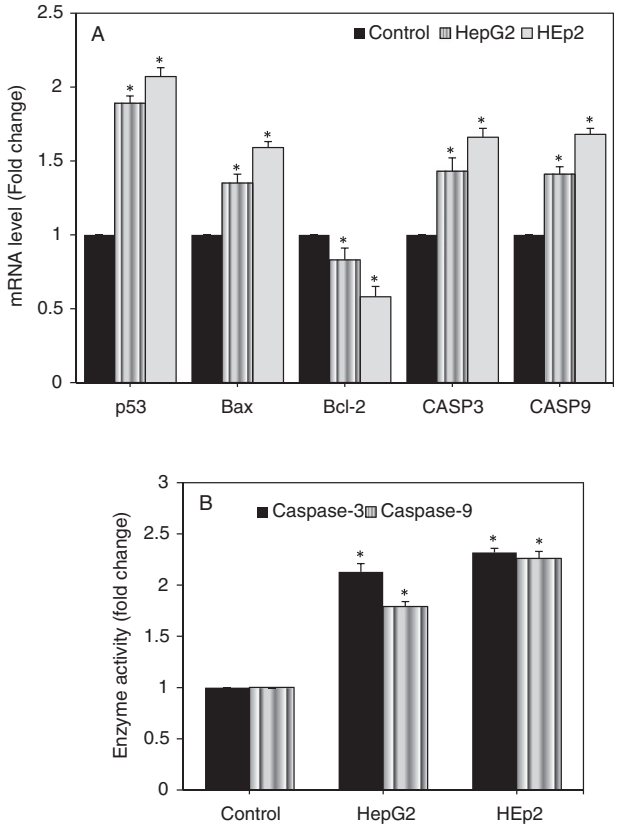

Figure 7. Dolomite nanoparticles (NPs) induced apoptosis in HepG2 and HEp2 cells. (A) Regulation of mRNA levels of apoptotic genes in HepG2 and HEp2 cells after exposure to dolomite NPs at a concentration of 40 μg ml^{-1} for 24 h. The mRNA levels were determined by quantitative real-time PCR as described in materials and methods. (B) Activity of caspase-3 and caspase-9 enzymes in HepG2 and HEp2 cells after exposure to dolomite NPs at a concentration of 40 μg ml^{-1} for 24 h. Data represented are the mean ± SD of three identical experiments made in three replicate. *Significant difference as compared with the controls (P <0.05 for each).

nature of this material. The hydrodynamic size of dolomite NPs in de-ionized and culture medium as determined by DLS was 287 and 237 nm, respectively. We observed that the hydrodynamic size of dolomite NPs was around 20 times higher as compared with the primary size. The higher size of NPs in aqueous suspension than the primary size could be due to tendency of NPs to agglomerate in aqueous suspension (Bai *et al*., 2009). That indicates the possible interaction of dolomite NPs with the protein of culture media, which has been widely reported with different NPs that leads to the formation of 'protein corona' (Lundqvist *et al*., 2008; Lynch and Dawson, 2008). Therefore, not only the size of the primary NPs but also the size of the secondary NPs could be used as a characteristic parameter to determine the *in vitro* toxicity of NPs in a cell culture medium (Avalos *et al*., 2014; Kato, 2011). The tendency of particles to form aggregates depends on the surface charge. The surface charge of dolomite NPs determined as zeta potential was −16 and −21 mV for de-ionized and culture medium, respectively.

After physiochemical characterization, a series of toxicological assays were performed to evaluate the *in vitro* cytotoxic effect of dolomite NPs on HEp2 and HepG2 cells and to understand the possible mechanisms of toxicity. We have employed more than one assay to evaluate the cytotoxic response of dolomite NPs. The cytotoxicity assays employed were mitochondrial function (MTT), lysosomal activity (NRU) and membrane integrity (LDH leakage). These assays served as sensitive and integrated measures of cell integrity and inhibition of cell proliferation. Normally, these assays are regularly utilized to examine the cytotoxic potential of various NPs in different cell lines (Ahamed and Alhadlaq, 2014; Avalos *et al*., 2014; Barillet *et al*., 2010; Mahmoudi *et al*., 2009; Sharma *et al*., 2009). These assays demonstrated that dolomite NPs induced cytotoxicity to HEp2 and HepG2 cells in a concentration-dependent manner in the dosage range of 10–80 μg ml^{-1}. Recently, Patil *et al*. (2012) reported that the minimum concentration of dolomite particles that cause significant cytotoxicity to human lung epithelial (A549) cells was around 100 μg ml^{-1}. However, in the present study, the minimum concentration required for dolomite particles to induce cytotoxicity in HEp2 and HepG2 cells was 10 μg ml–1.

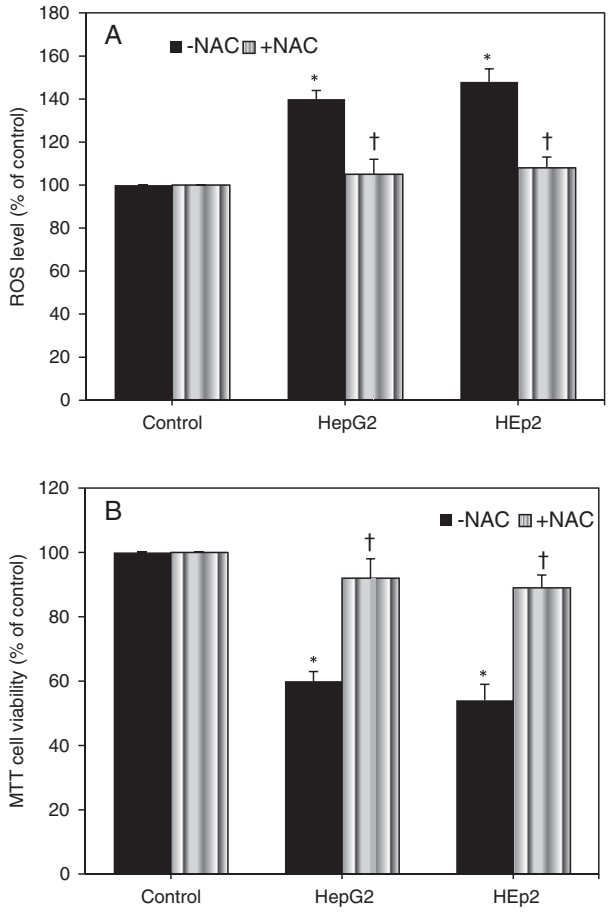

Figure 8. Dolomite nanoparticles (NPs) induced cytotoxicity in HepG2 and HEp2 cells through oxidative stress. Cells were exposed to dolomite NPs at a concentration of 40 μg ml^{-1} in the presence or 10 mM N-acetylcystein (NAC) 24 h. At the end of exposure reactive oxygen species (ROS) and mitochondrial function (MTT) assays were determined as described in the *Materials and methods*. (A) NAC significantly prevented the intracellular ROS generation in HepG2 and HEp2 cells caused by dolomite NPs. (B) NAC significantly preserved the viability (MTT assay) of HepG2 and HEp2 cells caused by dolomite nanoparticles. Data represented are the mean ± SD of three identical experiments made in three replicate. *Significant difference as compared with the controls ($P < 0.05$ for each). †Significant inhibitory effect of NAC on ROS generation and cell viability reduction caused by dolomite NPs ($P < 0.05$ for each).

This difference was expected, because an average size of our dolomite NPs (13 nm) was much lesser than the mean size of dolomite NPs (122 nm) used by Patil *et al*. (2012). This is also supported by other studies showing the greater toxic effects for smaller NPs (Cha *et al*., 2008; Elsaesser and Howard, 2012).

The MTT assay evaluates the ability of living cells mitochondria to reduce the soluble, yellow MTT into an insoluble, purple formazan. The reduction of MTT to formazan indicates the presence of living cells. A concentration-response dolomite NPs in HEp2 and HepG2 cells showed the decrease in the reduction of MTT to formazan with the increasing concentration. The NRU assay represents the lysosomal activity of cells, which is inhibited by dolomite NPs. Our MTT and NRU results are consistent with the observed low MMP in both HEp2 and HepG2 cells exposed to dolomite NPs. Disruption of mitochondria and lysosome functions along with low MMP suggested that dolomite NPs induced apoptosis in HEp2 and HepG2 cells through the mitochondrial pathway. A recent study suggested that mitochondrial events of apoptosis involve opening of a pore in the inner mitochondrial membrane, referred to as the mitochondrial permeability transition pore (MPTP) and MMP loss (Kitsis and Molkentin, 2010). Opening of the MPTP results in the mitochondrial swelling and rupture of the outer mitochondrial membrane during apoptosis. This subsequently results in the release of apoptogens that likely engage the components of the apoptosis machinery to further enhance cell death (Nicoletti *et al*., 1991; Ravi *et al*., 2010). Damage to the lysosomal membranes is known to release lysosome protease into intracellular spaces, which affects the neighbor cells, and triggers cell death as a result of apoptosis (Leist and Jaattela, 2001)

The concentration response of dolomite NPs to HEp2 cells in the LDH assay showed that with the increasing concentrations of dolomite NPs, more LDH was released to the culture medium, which indicated the membrane integrity was decreasing with the increasing concentrations of dolomite NPs. LDH leakage from cells is further evidence for both the penetration of NPs into cells and cell membrane damage (Hussain *et al*., 2005). LDH leakage in cell culture medium due to NPs exposure is also reported by other investigators (Ahamed, 2013; Akhtar *et al*., 2010; Kim *et al*., 2011; Patil *et al*., 2012; Yu *et al*., 2009).

It has been reported in the scientific literature that the general trend of NPs cytotoxicity is similar among various types of NPs (Jin *et al*., 2008) and that oxidative stress is one of the largest concerns in NPs cytotoxicity (Colvin, 2003; Nel *et al*., 2006; Xia *et al*., 2006). We also observed oxidant levels (ROS and lipid peroxidation) were significantly higher whereas the antioxidant GSH level was significantly lower in both HEp2 and HepG2 cells exposed to dolomite NPs. Furthermore, cytotoxicity induced by dolomite NPs was efficiently prevented by antioxidant NAC treatment (Fig. 8). These findings suggest that oxidative stress is primarily responsible for the cytotoxicity of dolomite NPs in both types of cells. A number of previous studies have implicated the production of ROS in cytotoxicity mediated by NPs (Foldbjerg *et al*., 2009; Hussain *et al*., 2005; Xia *et al*., 2006).

ROS and oxidative stress have been suggested to be involved in DNA damage and apoptosis (Ott *et al*., 2007). ROS generation, in particular, has also been associated with apoptosis in many conditions such as inflammation, ischemia, lung edema, neurodegeneration and cancer (Bai and Meng, 2005; Kannan and Jain, 2000). In the present study, we evaluated the regulation of mRNA of apoptotic genes in HEp2 and HepG2 cells. Results demonstrated that tumor suppressor gene p53 and pro-apoptotic gene bax were up-regulated, whereas the anti-apoptotic gene bcl-2 was down-regulated in both types of cells as a result of dolomite NPs exposure. It has been suggested that bax is up-regulated by p53 (Gopinath *et al*., 2010). As an increase in bax expression was observed, the role of p53 in the up-regulation of bax upon dolomite NPs exposure can be postulated. The insertion of bax into the mitochondrial membrane possibly leads to p53-mediated apoptosis (Gopinath *et al*., 2010). Caspases are activated during apoptosis in many cells and are known to play a vital role in both initiation and execution of apoptosis. It was reported that caspase-3 (CASP3) and caspase-9 (CASP9) are essential genes involved in cellular DNA damage and apoptosis (Janicke *et al*., 1998). We also observed that apoptotic genes CASP3 and CASP9 were up-regulated in dolomite NPs-treated cells. To confirm quantitative real-time PCR results this study further demonstrated that activity of caspase-3 and caspase-9 enzymes (protein expression) was higher in both

HEp2 HepG2 cells after dolomite NPs exposure. We have provided the evidence that dolomite NPs induced apoptosis, which was mediated through ROS via the p53 pathway in HEp2 and HepG2 cells. These results are in agreement with our previous studies where we found that various types of NPs induced apoptosis through ROS generation via p53, bax/bcl-2 and caspase pathways (Ahamed *et al*., 2008, 2012, 2014; Siddiqui *et al*., 2013).

Conclusion

We have shown that dolomite NPs induced cytotoxicity (MTT, NRU and LDH) to human larynx HEp2 and liver HepG2 cells in a concentration-dependent manner in the dosage range of 10–80 $\mu g\,ml^{-1}$. Dolomite was also found to induce oxidative stress in a concentration-dependent manner, as evidenced by depletion of glutathione and induction of the ROS level and lipid peroxidation. Cytotoxicity induced by dolomite NPs was efficiently prevented by N-acetyl-cysteine (ROS scavenger) suggesting that oxidative stress is the primarily cause of dolomite NPs cytotoxicity. Dolomite NPs-induced apoptosis is showed by loss of MMP and regulation of the apoptotic gene (p53, bax, bcl-2, CASP3 and CASP9). It is also worth mentioning that HEp2 cells seem to be marginally more susceptible to dolomite NPs exposure than HepG2 cells. Altogether, this study suggesting that dolomite NPs induced cytotoxicity, which is likely to be mediated through oxidative stress. Further investigations are underway to explore the toxicity mechanisms of dolomite NPs at an *in vivo* level.

Acknowledgements

The authors extend their appreciation to the Deanship of Scientific Research at King Saud University for funding this work through research group no.: RGP-VPP-308.

Conflict of Interest

The Authors did not report any conflict of interest.

References

Ahamed M. 2013. Silica nanoparticles induced cytotoxicity, oxidative stress and apoptosis in A549 and A431 cells. *Hum. Exp. Toxicol.* **32**:186–195.

Ahamed M, Alhadlaq HA. 2014. Nickel nanoparticle-induced dose-dependent cyto-genotoxicity in human breast carcinoma MCF-7 cells. *Onco. Targets Ther.* **7**:269–280.

Ahamed M, Karns M, Goodson M, Rowe J, Hussain S, Schlager J, Hong Y. 2008. DNA damage response to different surface chemistry of silver nanoparticles in mammalian cells. *Toxicol. Appl. Pharmacol.* **233**: 404–410.

Ahamed M, AlSalhi MS, Siddiqui MKJ. 2010. Silver nanoparticle applications and human health. *Clin. Chim. Acta* **411**:1841–1848.

Ahamed M, Akhtar MJ, Siddiqui MA, Ahmad J, Musarrat J, Al-Khedhairy AA, Alrokayan SA. 2011. Oxidative stress mediated apoptosis induced by nickel ferrite nanoparticles in cultured A549 cells. *Toxicology* **283**:101–108.

Ahmad J, Ahamed M, Akhtar MJ, Alrokayan SA, Siddiqui MA, Musarrat J, Al-Khedhairy AA. 2012. Apoptosis induction by amorphous silica nanoparticles mediated through reactive oxygen species generation in human liver cell line HepG2. *Toxicol. Appl. Pharmacol.* **259**:160–168.

Akhtar MJ, Ahamed M, Kumar S, Siddiqui S, Patil G, Ashquin M, Ahmad I. 2010. Nanotoxicity of pure silica mediated through oxidant generation rather than glutathione depletion in human lung epithelial cells. *Toxicology* **276**:95–102.

Akhtar MJ, Ahamed M, Khan MA, Alrokayan SA, Ahmad I, Kumar S. 2014. Cytotoxicity and apoptosis induction by nanoscale talc particles from two different geographical regions in human lung epithelial cells. *Environ. Toxicol.* **29**:394–406.

Avalos A, Haza AI, Mateo D, Morales P. 2014. Cytotoxicity and ROS production of manufactured silver nanoparticles of different sizes in hepatoma and leukemia cells. *J. Appl. Toxicol.* **34**:413–423.

Bai J, Meng Z. 2005. Effects of sulfur dioxide on apoptosis-related gene expressions in lungs from rats. *Regul. Toxicol. Pharmacol.* **43**:272–279.

Bai W, Zhang Z, Tian W, He X, Ma Y, Zhao Y, Chai Z. 2009. Toxicity of zinc oxide nanoparticles to zebrafish embryo: a physicochemical study of toxicity mechanism. *J. Nanopart. Res.* **12**:1645–1654.

Barillet S, Jugan ML, Laye M, Leconte Y, Herlin-Boime N, Reynaud C, Carriere M. 2010. *In vitro* evaluation of SiC nanoparticles impact on A549 pulmonary cells: cyto-, genotoxicity and oxidative stress. *Toxicol. Lett.* **198**:324–330.

Berasain C, Garcia-Trevijano ER, Castillo J, Erroba E, Santamaria M, Lee DC. 2005. Novel role for amphiregulin in protection from liver injury. *J. Biol. Chem.* **280**:19012–19020.

Berlo DV, Haberzettl P, Gerloff K, Li H, Scherbart AM, Albrecht C, Schins PF. 2009. Investigation of the cytotoxic and proinflammatory effects of cement dusts in rat alveolar macrophages. *Chem. Res. Toxicol.* **22**:1548–1558.

BGS (British Geological Survey) on Dolomites. 2006. Natural environment research council. *Mineral Planning Fact Sheet*. http://www.mineralsUK.com [accessed 26 August 2014].

Borenfreund E, Puerner JA. 1984. A simple quantitative procedure using monolayer cultures for cytotoxicity assays. *J. Tissue Cult Meth.* **9**:7–9.

Bradford MM. 1976. A rapid and sensitive method for the quantitation of microgram quantities of protein utilizing the principle of protein-dye binding. *Anal. Biochem.* **72**:248–254.

Buseck PR, Pósfai M. 1999. Airborne minerals and related aerosol particles: Effects on climate and the environment. *Proc. Natl. Acad. Sci. U. S. A.* **96**:3372–3379.

Cha K, Hong HW, Choi YG, Lee MJ, Park JH, Chae HK, Ryu G, Myung H. 2008. Comparison of acute responses of mice livers to short-term exposure to nano-sized or micro-sized silver particles. *Biotechnol. Lett.* **30**:1893–1899.

Chen GC, He ZL, Stoffella PJ, Yang XE, Yu S, Yang JY, Calvert DV. 2006. Leaching potential of heavy metals (Cd, Ni, Pb, Cu and Zn) from acidic sandy soil amended with dolomite phosphate rock (DPR) fertilizers. *J. Trace Elem. Med. Biol.* **20**:127–133.

Chougule M, Patel AR, Sachdeva P, Jackson T, Singh M. 2011. Anticancer activity of Noscapine, an opioid alkaloid in combination with cisplatin in human non-small cell lung cancer. *Lung Cancer* **71**:271–281.

Colvin VL. 2003. The potential environmental impact of engineered nanomaterials. *Nat. Biotechnol.* **21**:1166–1170.

Ellman GI. 1959. Tissue sulfhydryl groups. *Arch. Biochem. Biophys.* **82**:70–77.

Elsaesser A, Howard CV. 2012. Toxicology of nanoparticles. *Adv. Drug Deliv. Rev.* **69**:129–137.

Fahmy B, Cormier SA. 2009. Copper oxide nanoparticles induce oxidative stress and cytotoxicity in airway epithelial cells. *Toxicol. In Vitro* **23**:1365–1371.

Foldbjerg R, Olesen P, Hougaard M, Dang DA, Hoffmann HJ, Autrup H. 2009. PVP-coated silver nanoparticles and silver ions induce reactive oxygen species, apoptosis and necrosis in THP-1 monocytes. *Toxicol. Lett.* **190**:156–162.

Gopinath P, Gogoi SK, Sanpui P, Paul A, Chattopadhyay A, Ghosh SS. 2010. Signaling gene cascade in silver nanoparticle induced apoptosis. *Colloids Surf. B* **77**:240–245.

Guo C, Wang AY. 2009. Significance of increased apoptosis and bax expression in human small intestinal adenocarcinoma. *J. Histochem. Cytochem.* **57**:1139–1148.

Hochella MF, Lower SK, Maurice PA, Penn RL, Sahai N, Sparks DL, Twining BS. 2008, Nanominerals, mineral nanoparticles, and earth systems. *Science* **319**:1631–1635.

Hussain SM, Hess KL, Gearhart JM. 2005. In vitro toxicity of nanoparticles in BRL 3A rat liver cells. *Toxicol. In Vitro* **19**:975–983.

Janez S. 2001. "Žiga Zois in Déodat de Dolomieu". Kronika: časopis za slovensko krajevno zgodovino [*The Chronicle*: *the Newspaper for the Slovenian History of Places*] (in Slovene, with an English abstract) (Association of Slovenian Historical Societies, Section for the History of Places) **49**:65–72.

Janicke RU, Sprengart ML, Wati MR, Porter AG. 1998. Caspase-3 is required for DNA fragmentation and morphological changes associated with apoptosis. *J. Biol. Chem.* **273**:9357–9360.

Jin CY, Zhu BS, Wang XF, Lu QH. 2008. Cytotoxicity of titanium dioxide nanoparticles in mouse fibroblast cells. *Chem. Res. Toxicol.* **21**:1871–1877.

Johnston HJ, Hutchison GR, Christensen FM, Peters S, Hankin S, Stone V. 2009. Identification of the mechanisms that drive the toxicity of TiO_2 particulates: the contribution of physicochemical characteristics. *Part. Fibre Toxicol.* **6**:33.

Jos A, Pichardo S, Puerto M, Sánchez E, Gribo A, Camean AM. 2009. Cytotoxicity of carboxylic acid functionalized single wall carbon nanotubes on the human intestinal cell line Caco-2. *Toxicol. In Vitro* **23**:1491–1496.

Kannan K, Jain SK. 2000. Oxidative stress and apoptosis. *Pathophysiology* **7**:153–163.

Kato H. 2011. In vitro assays: Tracking nanoparticles inside cells. *Nat. Nanotechnol.* **6**:139–140.

Kim YS, Kim JS, Cho HS, Rha DS, Kim JM, Park JD, Choi BS, Lim R, Chang HK, Chung YH, Kwon IH, Jeong J, Han BS, Yu IJ. 2008. Twenty eight day oral toxicity, genotoxicity, and gender-related tissue distribution of silver nanoparticles in Sprague–Dawley rats. *Inhal. Toxicol.* **20**:575–583.

Kim HR, Kim MJ, Lee SY, Oh SM, Chung KH. 2011. Genotoxic effects of silver nanoparticles stimulated by oxidative stress in human normal bronchial epithelial (BEAS-2B) cells. *Mutat. Res.* **726**:129–135.

Kitsis RN, Molkentin JD. 2010. Apoptotic cell death nixed by an ER–mitochondrial necrotic pathway. *Proc. Natl. Acad. Sci. U. S. A.* **107**:9031–9032.

Leist M, Jaattela M. 2001. Four deaths and a funeral: From caspases to alternative mechanisms. *Nat. Rev. Mol. Cell Biol.* **2**:589–598.

Lundqvist M, Stigler J, Elia G, Lynch I, Cerdevall T, Dawson K. 2008. Nanoparticle size and surface properties determine the protein corona with possible implications for biological impacts. *Proc. Natl. Acad. Sci. U. S. A.* **105**:14265–14270.

Lynch I, Dawson K. 2008. Protein-nanoparticle interactions. *Nanotoday* **3**:40–47.

Madl AK, Pinkerton KE. 2009. Health effects of inhaled engineered and incidental nanoparticles. *Crit. Rev. Toxicol.* **39**:629–658.

Mahmood M, Casciano DA, Mocan T, Iancu C, Xu Y, Mocan L, Iancu DT, Dervishi E, Li Z, Abdalmuhsen M, Biris AR, Ali N, Howard P, Biris AS. 2010. Cytotoxicity and biological effects of functional nanomaterials delivered to various cell lines. *J. Appl. Toxicol.* **30**:74–83.

Mahmoudi M, Simchi A, Milani AS, Stroeve P. 2009. Cell toxicity of superparamagnetic iron oxide nanoparticles. *J. Colloid Interf. Sci.* **336**:510–518.

Maynard AD, Kuempel ED. 2005. Airborne nanostructured particles and occupational health. *J. Nanopart. Res.* **7**:587–614.

Maynard AD, Aitken RJ, Butz T, Colvin V, Donaldson K, Oberdorster G, Philbert MA, Ryan J, Seaton A, Stone V, Tinkle SS, Walker NJ, Warheit DB. 2006. Safe handling in nanotechnology. *Nature* **444**:267–269.

Medical Research. 2012. Study on Pulmonary Toxicity of Nanoparticles of Calcium Carbonate. http://www.res-medical.com/preventive-medicine/38466 [accessed 6 August 2014].

Mizoguchi T, Nagasawa S, Takahashi N, Yagasaki H, Ito M. 2005. Dolomite supplementation improves bone metabolism through modulation of calcium-regulating hormone secretion in ovariectomized rats. *J. Bone Miner. Metab.* **23**:140–146.

Mossman T 1983. Rapid colorimetric assay for cellular growth and survival: Application to proliferation and cytotoxicity assays. *J. Immunol. Methods* **65**:55–63.

Murdock RC, Braydich-Stolle L, Schrand AM, Schlager JJ, Hussain SM. 2008. Characterization of nanomaterial dispersion in solution prior to in vitro exposure using dynamic light scattering technique. *Toxicol. Sci.* **101**:239–253.

Nel A, Xia T, Madler L, Li N. 2006. Toxic potential of materials at the nanolevel. *Science* **311**:622–627.

Nicoletti I, Migliorati G, Pagliacci MC, Grignani F, Riccardi C. 1991. A rapid and simple method for measuring thymocyte apoptosis by propidium iodide staining and flow cytometry. *J. Immunol. Methods* **139**:271–279.

Oberdorster G, Oberdorster E, Oberdorster J. 2005. Nanotoxicology: an emerging discipline evolving from studies of ultrafine particles. *Environ. Health Perspect.* **113**:823–839.

Ohkawa H, Ohishi N, Yagi K. 1979. Assay for lipid peroxides in animal tissues by thiobarbituric acid reaction. *Anal. Biochem.* **95**:351–358.

Ott M, Gogvadze V, Orrenius S, Zhivotovsky B. 2007. Mitochondria, oxidative stress and cell death. *Apoptosis* **12**:913–922.

Patil G, Khan MI, Patel DK, Sultanad K, Prasad R, Ahmad I. 2012. Evaluation of cytotoxic, oxidative stress, proinflammatory and genotoxic responses of micro- and nano-particles of dolomite on human lung epithelial cells A549. *Environ. Toxicol. Pharmacol.* **34**:436–445.

Patlolla A, Patlolla B, Tchounwou P. 2010. Evaluation of cell viability, DNA damage, and cell death in normal human dermal fibroblast cells induced by functionalized multi walled carbon nanotube. *Mol. Cell. Biochem.* **338**:225–232.

Piret JP, Jacques D, Audinot JN, Mejia J, Boilan E. 2012. Copper (II) oxide nanoparticles penetrate into HepG2 cells, exert cytotoxicity via oxidative stress and induce pro-inflammatory response. *Nanoscale* **4**:7168–7184.

Plathe KL, Kammer F, Hassellöv M, Moore JN, Murayama M, Hofmann T, Hochella MF. 2013. The role of nanominerals and mineral nanoparticles in the transport of toxic trace metals: Field-flow fractionation and analytical TEM analyses after nanoparticle isolation and density separation. *Geochim. Cosmochim. Acta* **102**:213–225.

Ravi S, Chiruvella KK, Rajesh K, Prabhu V, Raghavan SC. 2010. 5-Isopropylidene-3-ethyl rhodanine induce growth inhibition followed by apoptosis in leukemia cells. *Eur. J. Med. Chem.* **45**:2748–2752.

Roberts RJ. 1981. Dolomite as a source of toxic metals. *N. Engl. J. Med.* **304**:423.

Sharma V, Shukla RK, Saxena N, Parmar D, Das M, Dhawan A. 2009. DNA damaging potential of zinc oxide nanoparticles in human epidermal cells. *Toxicol. Lett.* **185**:211–218.

Sharma V, Anderson D, Dhawan A. 2012. Zinc oxide nanoparticles induce oxidative DNA damage and ROS-triggered mitochondria mediated apoptosis in human liver cells (HepG2). *Apoptosis* **17**:852–870.

Sherr CJ. 2004. Principles of tumor suppression. *Cell* **11**:235–246.

Siddiqui MA, Ahamed M, Ahmad J, Khan MAM, Musarrat J, Al-Khedhairy AA, Alrokayan SA. 2012. Nickel oxide nanoparticles induce cytotoxicity, oxidative stress and apoptosis in cultured human cells that is abrogated by the dietary antioxidant curcumin. *Food Chem. Toxicol.* **50**:641–647.

Siddiqui MA, Alhadlaq HA, Ahmad J, Al-Khedhairy AA, Musarrat J, Ahamed M. 2013. Copper oxide nanoparticles induced mitochondria mediated apoptosis in human hepatocarcinoma cells. *PLoS One* **8**:e69534.

Slomski G, Odle T. "Dolomite." Gale Encyclopedia of Alternative Medicine. 2005. http://www.encyclopedia.com/doc/1G2-3435100269.html [last accessed 20 September 2014].

Wang H, Joseph JA. 1999. Quantifying cellular oxidative stress by dichlorofluorescin assay using microplate reader. *Free Radic. Biol. Med.* **27**:612–616.

Wang B, Feng W, Wang M, Wang T, Gu T, Zhu M, Ouyang H, Shi J, Zhang F, Zhao F, Chai Z, Wang H, Wang J. 2008. Acute toxicological impact of nano- and submicro-scaled zinc oxide powder on healthy adult mice. *J. Nanopart. Res.* **10**:263–276.

Xia T, Kovochich M, Brant J, Hotze M, Sempf J, Oberley T, Sioutas C, Yeh JI, Wiesner MR, Nel AE. 2006. Comparison of the abilities of ambient and manufactured nanoparticles to induce cellular toxicity according to an oxidative stress paradigm. *Nano Lett.* **6**:1794–1807.

Youle RJ, Strasser A. 2008. The BCL-2 protein family: opposing activities that mediate cell death. *Nat. Rev. Mol. Cell Biol.* **9**:47–59.

Yu KO, Grabinski CM, Schrand AM, Murdock RC, Wang W, Gu B, Schlager JJ, Hussain SM. 2009. Toxicity of amorphous silica nanoparticles in mouse keratinocytes. *J. Nanopart. Res.* **11**:15–24

Zhang Y, Jiang L, Jiang L, Geng C, Li L, Shao J, Zhong L. 2011. Possible involvement of oxidative stress in potassium bromate-induced genotoxicity in human HepG2 cells. *Chem. Biol. Int.* **189**:186–191.